A Biodegradable Injectable Implant Sustains Systemic and Ocular Delivery of an Aldose Reductase Inhibitor and Ameliorates Biochemical Changes in a Galactose-Fed Rat Model for Diabetic Complications

Jithan V. Aukunuru,[1,4] Gangadhar Sunkara,[1,4] Surya P. Ayalasomayajula,[1,4] Jack DeRuiter,[3] Randall C. Clark,[3] and Uday B. Kompella[1,2,5]

Received September 18, 2001; accepted November 28, 2001

Purpose. To fabricate and characterize *in vitro* and *in vivo* performance of a sustained release biodegradable implant for N-4-(benzoylaminophenylsulfonyl glycine) (BAPSG), a novel aldose reductase inhibitor.

Methods. The ability of BAPSG to inhibit aldose reductase activity and glucose-induced vascular endothelial growth factor (VEGF) expression was assessed in a retinal pigment epithelial cell line (ARPE-19). A poly (DL-lactic-co-glycolic acid) implant containing 50% w/w BAPSG was fabricated and characterized for drug loading, *in vitro* drug release, and the thermal behavior of the drug and the polymer. Implants were injected subcutaneously into a galactose-fed diabetic rat model and cataract scores, plasma and tissue drug levels, galactitol levels in the lens and the retina, glutathione levels in the plasma, lens, cornea and retina and VEGF expression in the retina were determined on or until 18 days.

Results. BAPSG inhibited aldose reductase activity and reduced VEGF expression in ARPE-19 cells. Implants (1 × 4 mm), with a loading efficiency of 106 ± 7% for BAPSG, were fabricated. Upon implant fabrication, while the glass transition temperature of the polymer decreased, the melting point of the drug was not affected. *In vivo* drug release correlated well with *in vitro* release, with ~44% drug release occurring *in vivo* by the end of 18 days. The implant reduced galactitol accumulation, glutathione depletion, cataract scores, and VEGF expression in galactose-fed rats.

Conclusions. An injectable biodegradable implant of BAPSG sustained drug release *in vitro* and *in vivo*, and reduced galactitol accumulation, glutathione depletion, cataract scores, and VEGF expression in galactose-fed rats.

KEY WORDS: aldose reductase inhibitor; ocular delivery; injectable implant; ARPE-19.

INTRODUCTION

Diabetic complications afflict over 124 million people worldwide (1). Although multiple biochemical pathways are likely responsible for the pathogenesis of diabetic complications, substantial evidence suggests a key role for aldose reductase pathway (2). In diabetic conditions, the enzyme aldose reductase converts excess glucose to sorbitol in a nicotinamide adenine dinucleotide phosphate (NADPH) dependent manner (3,4). Due to its poor membrane permeability, sorbitol accumulates in the cells, resulting in the disruption and death of the cells. Depletion of NADPH due to aldose reductase activity reduces intracellular glutathione (GSH), an endogenous antioxidant, thereby inducing oxidative stress, which is implicated in diabetic complications including retinopathy, nephropathy, neuropathy, and cataract formation (5). Indeed, inhibition of aldose reductase pathway with chronic oral administration of aldose reductase inhibitors (ARIs) has ameliorated diabetic complications in animal models and human subjects (6).

Several previously developed ARIs failed in clinical trials due to their non-selective enzyme inhibition, poor target tissue penetration, and toxicity (7). To overcome these problems, we synthesized benzoylaminophenylsulfonylglycine (BAPSG), an ARI with high enzyme specificity and good tissue penetration. Unlike several previously tested ARIs, BAPSG does not significantly inhibit genetically linked aldehyde reductase, catalytically similar oxidoreductases, or thymidylate synthase (8). The selectivity of BAPSG for aldose reductase compared to sorbinil and tolrestat, two established aldose reductase inhibitors, is very high. The IC_{50} values for rat aldose reductase are 0.4, 0.28, and 0.029 μM for BAPSG, sorbinil, and tolrestat, respectively (8). The corresponding values for rat aldehyde reductase are >100 (no significant inhibition even at 100 μM BAPSG), 1.9, and 0.54 μM, respectively. Thus, the selectivity index (IC_{50} for aldehyde reductase/ IC_{50} for aldose reductase) is >250, 7, and 19 for BAPSG, sorbinil and tolrestat, respectively. Furthermore, BAPSG accumulates in human retinal pigment epithelial cell cultures in a dose-dependent manner (9). For these reasons, BAPSG was chosen in this study.

In chronic diseases like diabetes, a prolonged delivery of drugs to the target tissues is required. Oral daily dosing is a common practice to treat such diseases. However, such dosing is associated with peaks at which drug could be toxic and troughs at which drug could be ineffective. A sustained release system can prolong the release of drugs at the site of action and reduce the fluctuations in drug levels, thereby rendering chronically administered drugs more safe, effective, and reliable (10). Therefore, this study developed a sustained release system for the delivery of BAPSG. Cylindrical implants and particulate systems are two common forms of biodegradable injectable drug delivery systems that can sustain the drug release. In this study, we used a cylindrical implant, as this system allows near 100% loading efficiency and also allows removal in case of any adverse effects. Previously, only one study assessed the sustained delivery of an aldose reductase inhibitor. Sorbinil, an aldose reductase inhibitor, was delivered to the lens by direct intracameral injection of the drug encapsulated in the liposomes using a mini osmotic pump (11). This delivery system sustained drug levels in the lens and

[1] Department of Pharmaceutical Sciences, University of Nebraska Medical Center, Omaha, Nebraska 68198-6025.
[2] Department of Ophthalmology, University of Nebraska Medical Center, Omaha, Nebraska 68198-6025.
[3] Department of Pharmacal Sciences, Auburn University, Auburn, Alabama 36849-5503.
[4] The first three authors contributed equally to the conduct of this work.
[5] To whom correspondence should be addressed. (e-mail: ukompell@unmc.edu)

0724-8741/02/0300-0278/0 © 2002 Plenum Publishing Corporation

failed to deliver drug to other ocular tissues. However, ARIs are desirable in systemic circulation as well as ocular tissues including cornea and retina and there are no previous reports on the usefulness of a sustained release system for the systemic and ocular delivery of an ARI.

Galactose-fed rat is a widely used model to examine the role of aldose reductase pathway in diabetic complications. Galactose, being a better substrate than glucose for aldose reductase, gets efficiently converted to galactitol, a polyol that rapidly accumulates in cells, similar to sorbitol (3). Galactose-fed rats develop cataract within a week of feeding and symptoms of diabetic retinopathy appear at the end of one-year (3,12). In these rats, the activation of aldose reductase pathway decreases cellular glutathione and enhances oxidative stress (30), a potent stimulus for the expression of vascular endothelial growth factor (VEGF), an endothelial mitogen suggested to play a role in retinal neovascularization in diabetic retinopathy (12,13). Indeed, Frank *et al.* (12) observed that chronic oral ARI therapy reduces VEGF protein in the retinas of galactose fed rats. The current study, for the first time, will assess VEGF expression following short-term treatment with ARI in a galactose-fed rat model.

ARI therapy, besides preventing or delaying cataracts and diabetic retinopathy, is likely to prevent or delay other systemic complications including nephropathy and neuropathy (5). Thus, maintaining plasma concentrations of BAPSG would benefit both ocular and systemic diabetic complications. Topical, vitreal, and systemic administrations are three possible modes of delivery for this molecule. Topical administration, apart from not providing adequate plasma drug levels, is unlikely to deliver drug to the posterior segment of the eye (14). Intravitreal administration, a direct mode of drug delivery to the retina, apart from being invasive, would not result in adequate systemic levels of BAPSG. Oral daily dosing is a common practice to treat chronic diseases like diabetes. However, such dosing is associated with peaks at which the drug could be toxic and troughs at which the drug could be ineffective. Another limitation of this route is the poor bioavailability (~6%) of BAPSG following oral administration (15). Although blood-retinal and blood-aqueous barriers are formidable, some drugs reach intraocular tissues including retina and lens from systemic circulation (16). As BAPSG has low oral bioavailability and near complete absorption from subcutaneous route (15), this study assessed subcutaneous route for systemic and ocular delivery of BAPSG.

Subcutaneous biodegradable implants were previously tested successfully in contraception, cancer chemotherapy, analgesia in chronic pain, and growth factor delivery (10). Because of favorable absorption and easy removability, subcutaneous route is one of the most used routes of implant administration. These implants sustain drug levels in the plasma and reduce the fluctuations. Although subcutaneous route of drug delivery to various tissues was previously assessed, sustained retinal drug delivery through systemic mode of administration was not addressed. Thus, the objective of this study was to fabricate an injectable biodegradable implant of a novel aldose reductase inhibitor and to assess its *in vivo* ability to achieve ocular tissue BAPSG levels, reduce galactitol accumulation, glutathione depletion, cataract scores, and VEGF expression in a galactose-fed rat model after subcutaneous administration.

MATERIALS AND METHODS

Cell Culture Studies

A human retinal pigment epithelial (ARPE-19) cell line was used in this study. Unless otherwise stated, ARPE-19 cells obtained from ATCC (Rockville, Maryland) were grown as described elsewhere (9). ARPE-19 cells were used between passages 19 and 29.

In Vitro Activity of BAPSG in ARPE-19 Cells

To determine the aldose reductase inhibitory activity of BAPSG (MW: 334.35), ARPE-19 cells were grown in galactose (30 mM) containing DMEM/F12 medium with 10% FBS for 30 days with and without BAPSG. At the end of this period, the cells were lysed and galactitol was estimated using a gas chromatography (GC) method. For the GC analysis, the cell lysates were spiked with the internal standard, α-methyl-D-mannopyranoside (50 μl of 2 mg/ml preparation), and homogenized. Proteins in the homogenate were precipitated by adding ice-cold ethanol. The supernatant was lyophilized and silylated with Tri-Sil "Z" (Trimethylsilyl imidazole; Pierce Chemical Co., Ltd., Rockford, Illinois) by heating at 60 ± 2°C for 1 h in a water bath. One microliter of the sample was injected onto Varian GC (Model 3700) equipped with a fused silica capillary column (30 m, 0.53 mm i.d., and 1.5 μm film). The samples were analyzed using helium as a carrier gas with the following operating conditions: injector temperature, 250°C; flame ionization detector (FID) temperature, 270°C; column oven temperature, 100–220°C, varied at the rate of 6°C/min. The recovery of the internal standard and galactitol was 100% in this method and the limit of quantitation for galactitol was 30 nmol.

To determine the effect of BAPSG on VEGF expression, ARPE-19 cells were grown in low glucose (5 mM) DMEM/F12 medium with 1% FBS for 3 days. On day 4, the culture medium was removed and the cells were exposed to serum-free medium containing 5 mM glucose for 24 hrs in the presence and absence of BAPSG. At the end of this period, the media was replaced with 35 mM glucose containing serum-free medium in the presence and absence of BAPSG. After 12 h of incubation, VEGF secretion over an additional 12 h into serum-free medium containing 35 mM glucose was determined using an ELISA method capable of detecting $VEGF_{165}$ and $VEGF_{121}$ (Research Diagnositics Inc., Flanders, New Jersey). In addition, VEGF mRNA inside the cells was determined using a reverse transcriptase polymerase chain reaction (RT-PCR) (Promega Corporation, Madison, Wisconsin). Total RNA was extracted from ARPE-19 monolayers using RNA STAT-60™ RNA isolation kit (TEL-TEST, Friendswood, Texas). RT-PCR was performed as described by Boldrini *et al.* (17). The amplified products were separated on a 2% agarose gel and VEGF mRNA was quantified using densitometry analysis. This method is capable of detecting mRNAs of all five human VEGF isoforms.

Fabrication and Characterization of the Implant

Poly(DL-lactide-co-glycolic acid) (PLGA 85:15) of inherent viscosity, 0.65 dL/g (in methylene chloride at 30°C) (Birmingham Polymers Inc., Birmingham, Alabama), was used in the fabrication of an implant containing 50% w/w of

BAPSG. Initially, equal amounts of drug and polymer were dispersed in ethyl acetate:ethanol (6:1) mixture. This preparation was taken in a china crucible and the solvents evaporated to form a drug-polymer layer on the surface. This layer was scraped, powdered, and filled in a teflon tubing with an internal diameter of 1 mm and an external diameter of 2 mm. The tubing with the mixture was placed for 5 s in a furnace maintained at 150°C to form a melt, which was compressed and extruded using steel rods and cut to desired size.

To determine the drug loading in the implants, each implant was solubilized in methylene chloride and BAPSG was extracted into 5 ml of aqueous phase, an aliquot of which was injected onto HPLC for quantifying BAPSG. The thermal behavior of the drug and the polymer was determined using a differential scanning calorimeter (DSC-50, Shimadzu). For DSC, samples (4 mg each) of BAPSG, PLGA, BAPSG and PLGA mixture I (physical mixture of BAPSG and PLGA), BAPSG and PLGA mixture II (mixture obtained by dispersing BAPSG and PLGA in ethylacetate:ethanol (6:1) and evaporating the solvent), and BAPSG implant were heated from 30 to 300°C in an aluminum pan at a heating rate of 10°C/min in a N_2 atmosphere. Instrument calibration was performed using indium standard.

To determine *in vitro* drug release from the implants, implants were placed in a 2 ml vial containing 1 ml phosphate buffered saline (PBS) (pH 7.4) maintained at 37°C in a shaking water bath. The entire release medium was removed at the end of each time point and replaced with fresh medium. The samples were stored at –20° C until HPLC analysis of BAPSG (14).

In Vivo Release and Ocular Tissue Levels of BAPSG after Implant Administration in a Galactose-Fed Rat Model

To determine the *in vivo* efficacy of the implant, a galactose-fed rat model was used in these studies. Male Sprague-Dawley rats (~200 g) were randomized into three groups. Normal diet: Rats receiving normal diet (Purina, Inc., Richmond, Indiana); galactose diet: Rats receiving 50% galactose diet (50% w/w with normal diet); galactose diet with implants: Rats receiving 50% galactose diet with BAPSG implants (subcutaneous injection of four implants containing a total of 10 mg of BAPSG). Body weights of the rats were measured every day. To determine the galactosemic state of the rats, the percent total glycated hemoglobin (%GHb) in the rat blood was measured on day 7, 14, and 18 using an affinity column chromatography (Glyc-Affin; Perkin-Elmer Wallace, Inc., Norton, Ohio) based assay (18). The research with the rats adhered to the "Principles of Laboratory Animal Care" (NIH publication # 85-23, revised 1985).

To assess the ability of BAPSG implant to sustain drug release *in vivo*, four implants containing 50% w/w BAPSG (10 mg of BAPSG) were injected subcutaneously in the middle dorsal area of each galactose-fed rat with the help of a 16-guage needle. Intraperitoneal sodium pentobarbital at a dose of 40 mg/kg was given to anesthetize the rats prior to implant administration. The plasma was collected periodically and stored at –70°C until assayed for BAPSG. On day 18 after the implant administration, the rats were sacrificed using 200 mg/kg of intraperitoneal sodium pentobarbital and retina, cornea and lens were isolated from both the eyes. The tissues were homogenized in PBS. BAPSG in plasma and tissues was extracted and estimated using a HPLC method (10). Tissue recovery of BAPSG was 95% and the method was reproducible with inter-day relative standard deviation of <7%. The limit of detection and the limit of quantification for BAPSG were 1 and 25 ng, respectively. For comparative purposes, an equivalent bolus solution dose of BAPSG was administered subcutaneously into another group of rats. The plasma was collected periodically and stored at –70°C until assayed for BAPSG.

The fraction of drug absorbed *in vivo* from the implant was determined using the equation (19):

$$Ab/Ab^{\infty} = (C_p + K[AUC]_0^t)/K[AUC]_0^{\infty}$$

where, Ab is the amount of drug absorbed from time 0 to t, Ab^{∞} is the total amount of drug absorbed, C_p is the plasma concentration at time t, K is the elimination rate constant, AUC is the area under the curve. K and $[AUC]_0^{\infty}$ were determined after an equivalent subcutaneous dose of BAPSG. K was confirmed using intravenous data. The elimination rate constant of BAPSG was 0.82 h^{-1} and its bioavailability after subcutaneous administration was 98% (15).

Measurement of Biologic End Points after Implant Administration

Cataracts were scored in galactose-fed rats with or without BAPSG implant a before treatment, on day 7, and on day 18. After pupil dilation with 1% Mydriacyl, rats were examined using an ophthalmoscope. A certified ophthalmic photographer, who was blinded to the study design, evaluated the cataract scores. Cataracts were scored on a scale of 0–4 according to the degree of opacification (0: normal, clear lens; 1: posterior subcapsular opacity without anterior cortical opacity; 2: posterior opacity with vacuoles; 3: posterior opacity with slight anterior cortical opacity; 4: complete anterior opacity), as described previously (20).

Galactitol levels in the lens and retinal homogenates were estimated as per the method described above for the estimation of galactitol in ARPE-19 cells. Total glutathione in the cornea, lens, plasma and retina were estimated using a fluorimetric method as described previously (21). Following total RNA extraction, retinal VEGF mRNA was estimated using RT-PCR employing primers capable of detecting all five rat VEGF isoforms (22).

Statistical Analysis

The results are expressed as mean ± s.d. Student's *t*-test was used to evaluate the significance of differences between groups. $P < 0.05$ was considered statistically significant.

RESULTS

BAPSG Reduces Polyol Levels and VEGF Expression in ARPE-19 Cells

Compared to controls, BAPSG significantly reduced galactitol levels in ARPE-19 cell lysates by 54% (Fig. 1A). Upon exposure of BAPSG to ARPE-19 cells under high glucose conditions, VEGF secretion was significantly reduced by 26% (Fig. 1A). The RT-PCR analysis indicated a band at 584 bp, corresponding to $VEGF_{165}$, whose intensity was reduced by 27%, in the presence of BAPSG (Fig. 1B, 1C).

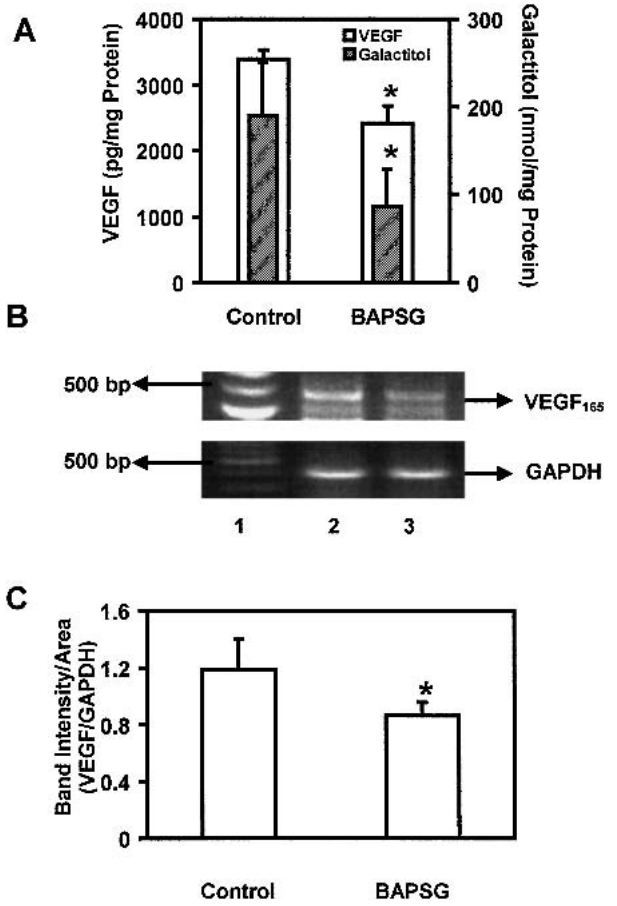

Fig. 1. BAPSG inhibits aldose reductase activity and VEGF expression and secretion in a human retinal pigment epithelial cell line (ARPE-19). A) Intracellular galactitol levels and VEGF secretion from ARPE-19 cells. Data is expressed as mean ± s.d for n = 4. *$P < 0.05$ vs. controls. B) VEGF mRNA expression in ARPE-19 cells. Key: 1. Molecular weight markers, 2. Control, 3. BAPSG. C) VEGF mRNA levels quantified as the relative band intensities of VEGF mRNA and GAPDH mRNA. Data is expressed as mean ± s.d. for n = 3. *$P < 0.05$ vs. controls.

Implant Fabrication and *in Vitro* Characterization

Using a melt-extrusion technique at 150°C, 1 × 4 mm cylindrical implants were fabricated. HPLC assay for the drug content indicated a loading of 106 ± 7% of the theoretical loading for BAPSG and no degradation products were detected. DSC thermograms indicated a decrease in glass transition temperature of the polymer upon fabrication (Fig. 2). The glass transition temperature of the polymer was 54 ± 0.3, 50 ± 1.5, 49 ± 1.2°C in PLGA (85/15), BAPSG & PLGA mixture II and the implant, respectively. However, fabrication did not affect the melting point of BAPSG. The melting temperature of BAPSG was 233 ± 0.8, 229 ± 2, and 230 ± 2°C with BAPSG, BAPSG & PLGA mixture II and the implant, respectively. The above glass transition and melting temperatures are expressed as mean ± s.d. for n = 3.

As seen in the SEM pictures of the implant before administration, the implant was about 4 mm long and 1 mm in diameter with smooth, straight sides with no visible pits or cracks at both the magnifications tested (Fig. 3A, 3B).

The cumulative amount of BAPSG released from the

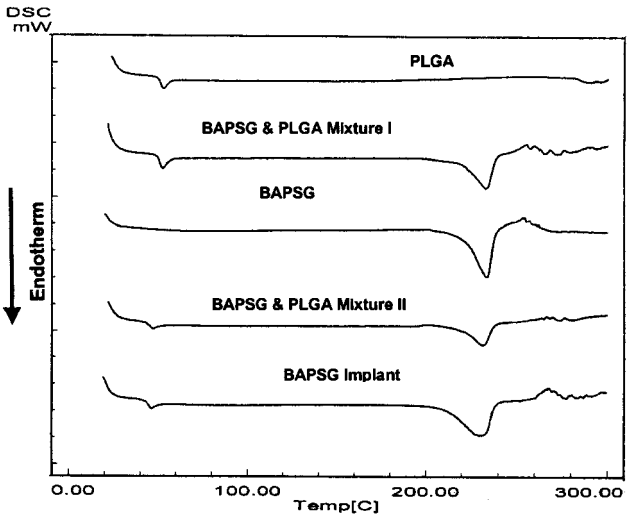

Fig. 2. Representative thermograms of the implant and its components. BAPSG & PLGA mixture I represents physical mixture of BAPSG and PLGA. BAPSG & PLGA mixture II represents the mixture of the drug and the polymer obtained by dispersing the two in a solvent and evaporating it.

implants is shown in Fig. 4B. The drug release was sustained during the study period, with 33% of the drug released by the end of 18 days.

In Vivo Drug Release from the Implant

The body weights were lower for the galactose-fed rats compared to controls at the end of 18 days of feeding. Similar decrease in body weight following galactose diet was reported

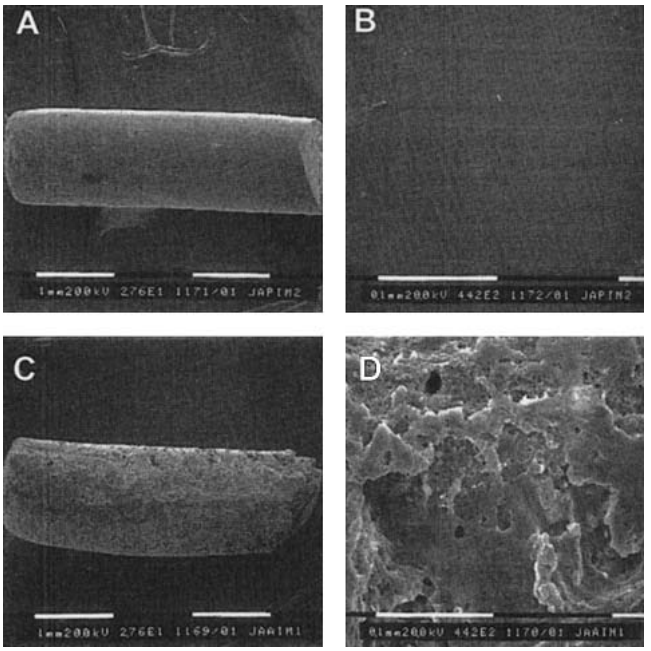

Fig. 3. SEM pictures of BAPSG implant. A) Implant before administration (27.6× magnification), B) Implant before administration (442× magnification), C) Implant retrieved from the animal on day 18 after administration (27.6× magnification), D) Implant retrieved from the animal on day 18 after implantation (442× magnification). Bar: 1 mm in panels A and C and 0.1 mm in panels B and D.

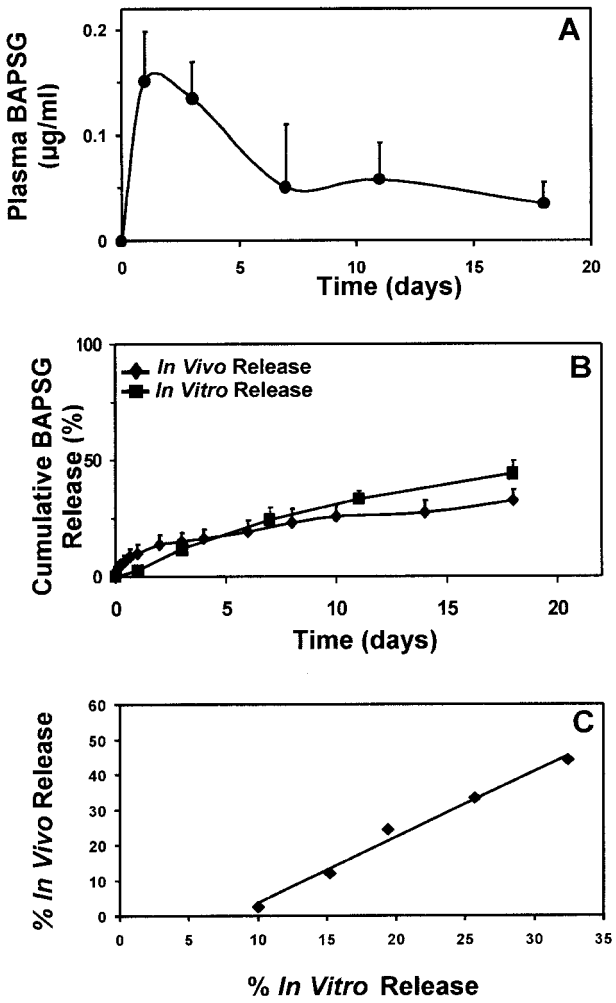

Fig. 4. A) Subcutaneous BAPSG-PLGA implant sustains plasma levels of BAPSG in galactose-fed rats. B) BAPSG release *in vitro* and *in vivo*. C. *In vitro-in vivo* correlation for BAPSG release. Data is expressed as mean ± s.d. for n = 4 or 5.

by Frank *et al.* (12) and Roy and Lorenzi (18). Compared to rats fed with normal diet, total %GHb was significantly higher in galactose and implant groups at all times of estimation (Table IA).

BAPSG rapidly disappeared from plasma after bolus subcutaneous administration and very low drug levels (<40 pg/ml) were detected in the plasma at the end of 24 h (data not shown). On the other hand, the single subcutaneous injection of the BAPSG implant produced plasma concentrations in the range of 0.05–0.15 µg/ml from day 1 through day 18, demonstrating sustained release of BAPSG in plasma following implant administration (Fig. 4A). The cumulative percent of BAPSG released from the implants is shown in Fig. 4B. The *in vivo* drug absorption was sustained during the study period with the cumulative amount released being 44% at the end of 18 days.

Table IA. Percent Total Glycated Haemoglobin

Treatment	% Glycated haemoglobin		
	7	14	18
Normal feed	4.6 ± 0.4	5.1 ± 0.4	5.1 ± 0.8
Galactose feed	6.5 ± 0.3[a]	8.2 ± 0.4[a]	7.1 ± 0.8[a]
Galactose feed + BAPSG implant	7.0 ± 0.3[a]	7.5 ± 0.3[a]	6.2 ± 0.2[a]

[a] $P < 0.05$ vs. normal feed, $p < 0.05$ *vs.* galactose feed.

Table IB. Cataract Scores

Treatment	Day of the scoring		
	0	7	18
Normal feed	0	0.3 ± 0.4	0.6 ± 0.7
Galactose feed	0	2.6 ± 0.8[a]	3.5 ± 0.5[a]
Galactose feed + BAPSG implant	0	0.9 ± 1.1[b]	2.6 ± 0.5

[a] $P < 0.05$ vs. normal feed, [b] $P < 0.05$ vs. galactose feed.

Besides the plasma, the implant sustained BAPSG levels in the ocular tissues (Fig. 5). On day 18, the drug levels in cornea, lens and retina were 2.2 ± 2.56, 0.5 ± 0.67 and 3.73 ± 2.39 µM (assuming 1 gm tissue = 1 cc), respectively. These levels likely reflect the bound plus free drug. The implant retained in the animal for 18 days exhibited an eroded surface with pits and cracks, suggesting drug release and degradation of the polymer *in vivo* (Fig. 3C, 3D).

Efficacy of the Implant in Galactose-fed Rat

The implant reduced the galactitol levels in the retina and lens of galactose-fed rats by 45 and 48%, respectively (Fig. 6A; $P < 0.05$). Galactose diet significantly reduced GSH levels in retina, lens, cornea, as well as plasma (Fig. 6B, 6C; $P < 0.05$). Total glutathione in plasma, cornea, lens and retina were decreased by 43, 45, 67, and 54%, respectively, in galactose-fed rats compared to normal rats (Fig. 6B, 6C; $P < 0.05$). In plasma, cornea, lens and retina, there was a significant reduction in this glutathione depletion upon implant administration.

At the end of 7 days, while galactose diet resulted in high cataract scores, these scores were significantly lower in the implant group (Table IB) ($P < 0.05$). However, at the end of 18 days, the cataract scores of the implant group, although less than the scores in galactose group, were not statistically different.

The RT-PCR amplified products separated on a 2% agarose gel demonstrated a band at 462 bp corresponding to the

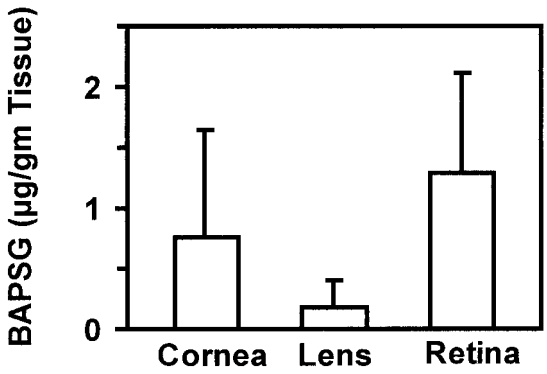

Fig. 5. Ocular tissue levels of BAPSG following a single subcutaneous implant administration in galactose-fed rats. Data is expressed as mean ± s.d. for n = 4.

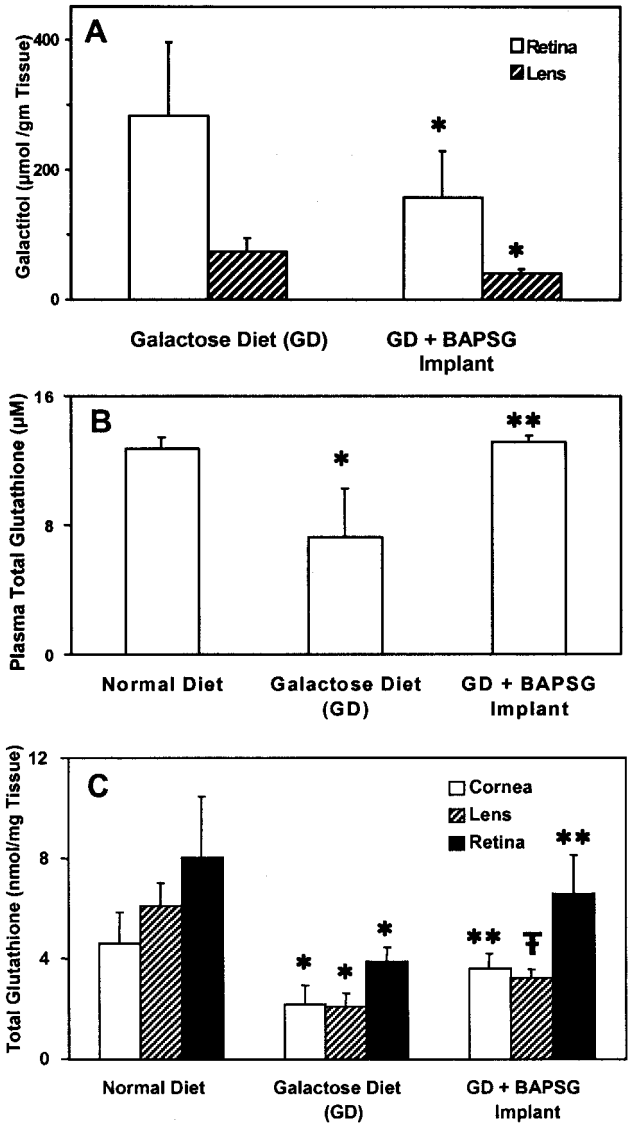

Fig. 6. *In vivo* effectiveness of BAPSG-PLGA implant on day 18 following galactose feeding. A) Inhibition of galactitol accumulation in ocular tissues by BAPSG implant. $*P < 0.05$ vs. untreated galactose diet group B) Reversal of plasma glutathione depletion by BAPSG implant. $*P < 0.05$ normal vs. untreated galactose diet group, $**P < 0.05$ implant group vs. untreated galactose diet group. C) Reduction of ocular tissue glutathione depletion by BAPSG implant. $*P < 0.05$ normal vs. untreated galactose diet group, $**P < 0.05$ implant group vs. untreated galactose diet group, $P < 0.10$ implant group vs. untreated galactose diet group, $P < 0.05$ implant groups vs. normal diet group.

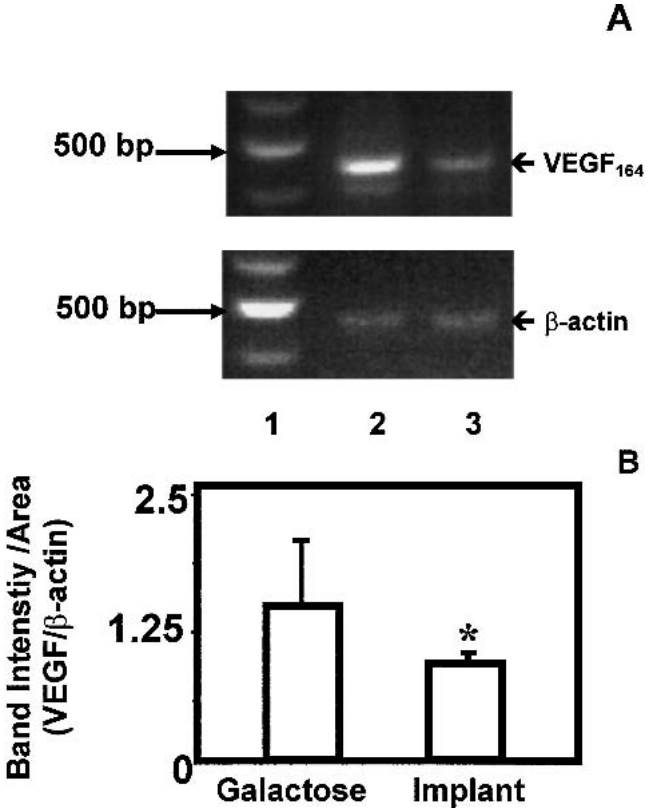

Fig. 7. Inhibition of VEGF expression in retina on day 18 following a single subcutaneous administration of BAPSG-PLGA implant. The retinas of rats were isolated at the end of 18 days. A) VEGF mRNA determined using RT-PCR. Key: 1. Molecular weight markers, 2. Galacotse, 3. BAPSG. B) VEGF mRNA levels quantified as the relative band intensities of VEGF mRNA and β–actin mRNA. Data is expressed as mean ± s.d. for n = 4 or 5.

mRNA of rat $VEGF_{164}$ (Fig. 7A). BAPSG implant significantly reduced the intensity of this band by 32% (Fig. 7B).

DISCUSSION

Although aldose reductase inhibitory activity of BAPSG was previously determined using a rat lens assay (8), its aldose reductase inhibitory activity in retinal cells was not determined. Pericytes and retinal pigment epithelial cells in retina express high aldose reductase activity and aldose reductase inhibitors were previously shown to reduce this activity (23,24). In this study, we used a retinal pigment epithelial cell line, ARPE-19, to determine the aldose reductase inhibitory activity of BAPSG in retinal cells. ARPE-19 cells have structural and functional characteristics similar to human retinal pigment epithelial (RPE) cells *in vivo* (25). Upon incubation with galactose, a substrate for aldose reductase, galactitol accumulated in ARPE-19 cells, consistent with the presence of aldose reductase activity in these cells. This is the first report indicating aldose reductase activity in ARPE-19 cells. The galactitol accumulation upon galactose exposure was significantly reduced by BAPSG, consistent with ARI activity of BAPSG (Fig. 1A). Previous studies with other ARIs obtained similar results using primary bovine retinal pigment epithelial cells (26).

In addition to inhibiting polyol accumulation, BAPSG decreased the secretion and expression of VEGF in ARPE-19 cells grown under high glucose conditions (Fig. 1B). VEGF is a potent endothelial mitogen implicated in retinal neovascularization associated with diabetic retinopathy and other vasoproliferative retinal disorders in humans and animals (13). Consistent with previous results with primary RPE cultures (27), there was an increase in the expression and secretion of VEGF in ARPE-19 cells on exposure to high glucose conditions. However, there are no previous cell culture studies reporting the inhibition of VEGF by aldose reductase inhibitors. We observed that BAPSG significantly reduced the expression and secretion of VEGF under high glucose

conditions, consistent with a role for polyol pathway in glucose-induced elevation of VEGF expression.

We fabricated small size biodegradable implants of BAPSG (Fig. 3A and 3B) that can possibly be injected by various routes including local administration in the eye (28). Following implant formation, the Tg of the polymer decreased (Fig. 2), consistent with the formation of a molecular dispersion of the drug in the polymer (29). We did not measure the residual solvent in the implant, which can possibly affect the implant's performance and quality. However, in the process of fabrication, ethylacetate mixture was evaporated at 55°C for 2 h followed by 5 s exposure to 150°C, possibly aiding in the complete removal of ethyl acetate. After subcutaneous administration, the implant sustained plasma (Fig. 4A) and ocular tissue levels of BAPSG (Fig. 5) and the *in vivo* absorption correlated well with *in vitro* release (Fig. 4C). Thus, subcutaneous administration of BAPSG implant will likely be useful in preventing or delaying systemic as well as ocular diabetic complications.

The BAPSG implant significantly reduced cataract scores on day 7 but not on day 18 (Table I), possibly because plasma levels were lower at later times following an initial burst of drug release from the implants (Fig. 4A). On day 18, at 35% of its *in vitro* IC_{50} concentration (0.4 μM) in rat plasma, BAPSG inhibited lens opacities and reduced retinal and lens galactitol concentrations by 45 and 48% (Fig. 7C), respectively, suggesting its superior *in vivo* efficacy.

Apart from polyol accumulation, aldose reductase pathway results in hypoxia like metabolic changes in the retina. Both polyol accumulation and hypoxia are known to enhance oxidative stress (4), a potent stimulus for VEGF (13). Only one previous study assessed the influence of aldose reductase inhibitors on VEGF protein levels in the retina (12). In a galactose fed rat model, at the end of one year of galactose feeding, VEGF levels in retina were elevated and this elevation was decreased in the rats fed with aldose reductase inhibitors along with the diet from the beginning. However, this previous study was a long-term study and there are no reports on VEGF expression after short-term ARI treatment. Oxidative stress appears very early in retina in diabetic and galactosemic models (3,4). We observed a reduction of glutathione, an oxidative stress marker, in the plasma, retina, lens and cornea in day 18 galactose-fed rats, indicating an elevation of oxidative stress in these tissues. BAPSG implant reduced glutathione depletion in plasma and ocular tissues at the end of 18 days, suggesting the ability of BAPSG to reduce oxidative stress in galactose-fed rat model. Interestingly, the reversal of glutathione levels as well as galactitol reduction correlated well with the tissue concentrations of the drug. Drug levels and glutathione reversal were in the order: retina>cornea>lens. Similarly, the inhibition of galactitol was greater in the retina compared to the lens. Oxidative stress, a potent stimulus for the expression of VEGF is a balance between oxidants and antioxidants. The levels of glutathione, a cellular antioxidant, decrease in the cell with an elevation of oxidative stress. Possibly for this reason, at the end of 18 days, BAPSG implant reduced the retinal VEGF mRNA levels. This is the first study suggesting a decrease in retinal VEGF expression upon short-term treatment with an aldose reductase inhibitor.

Taken together, the results of this study indicate that a subcutaneous BAPSG implant is capable of sustaining the release of BAPSG into the systemic circulation and ocular tissues. This is the first study to demonstrate the delivery of drugs to the ocular tissues using a sustained release systemic implant delivery system. Furthermore, this study demonstrated the efficacy of the BAPSG implant in normalizing short-term end-points in a galactose-fed rat model. Cataracts and biochemical changes like accumulation of galactitol and depletion of glutathione appear early in diabetic and galactosemic animal models and symptoms of diabetic retinopathy take longer periods for manifestation (3,12,30). The BAPSG implant reduced cataracts, galactitol accumulation, and glutathione depletion, indicating its ability to ameliorate diabetic complications. Furthermore, the implant partly decreased VEGF mRNA in the retina, indicating the potential value of BAPSG in reducing VEGF mediated neovascularization in diabetic retinopathy. Since VEGF is a major growth factor implicated in diabetic retinopathy, the decrease in the expression of VEGF mRNA is an important finding of this study. Longer studies with ARI implants will be conducted in future to understand the definitive role of aldose reductase inhibitors in the therapy of diabetic retinopathy. The findings of this study would open a new chapter of drug delivery strategies for ARI therapy for secondary diabetic complications, in order to improve the ARI risk-benefit ratio.

ACKNOWLEDGMENTS

The authors are grateful to Mr. Allen Katz, Certified Photographer at the Department of Ophthalmology, University of Nebraska Medical Center, for evaluating the cataract scores in the rats.

REFERENCES

1. L. Quinn. Type 2 diabetes: epidemiology, pathophysiology, and diagnosis. *Nurs. Clin. North Am.* **36**:175–192 (2001).
2. T. Nishikawa, D. Edelstein, and M. Brownlee. The missing link: a single unifying mechanism for diabetic complications. *Kidney Int.* **77**:S26–30 (2000).
3. P. F. Kador, J. Ioue, E. F. Secchi, M. J. Lizak, L. Rodriguez, K. Mori, W. Greentree, K. Blessing, P. A. Lackner, and S. Sato. Effect of sorbitol dehydrogenase inhibition on sugar cataract formation in galactose-fed and diabetic rats. *Exp. Eye Res.* **67**:203–208 (1998).
4. I. G. Obrosova, M. J. Stevens, and H. J. Lang. Diabetes-induced changes in retinal NAD-redox status: Pharmacological modulation and implications for pathogenesis in diabetic retinopathy. *Pharmacology* **62**:172–180 (2001).
5. L. Costantino, G. Rastelli, P. Vianello, G. Cignarella, and D. Barlocco. Diabetes complications and their potential prevention: aldose reductase inhibition and other approaches. *Med. Res. Rev.* **19**:3–23 (1999).
6. P. J. Oates and B. L. Mylari. Aldose reductase inhibitors: therapeutic implications for diabetic complications. *Expert. Opin. Investig. Drugs* **8**:2095–2119 (1999).
7. M. A. Pfeifer, M. P. Schumer, and D. A. Gelber. Aldose reductae inhibitors: the end of an era or the need for different trial designs? *Diabetes* **46**:S82–89 (1997).
8. R. A. Davis, C. A. Mayfield, J. L. Aull, and J. DeRuiter. Enzyme selectivity analysis of arylsulfonylamino acid aldose reductase inhibitors. *J. Enzyme Inhib.* **7**:87–96 (1993).
9. J. V. Aukunuru, G. Sunkara, N. Bandi, W. B. Thoreson, and U. B. Kompella. Expression of multidrug resistance-associated protein (MRP) in human retinal pigment epithelial cells and its interaction with BAPSG, a novel aldose reductase inhibitor. *Pharm. Res.* **18**:565–572 (2001).
10. A. K. Dash and G. C. Cudworth. Therapeutic applications of implantable drug delivery systems. *J. Pharmacol. Toxicol. Methods* **40**:1–12 (1998).
11. J. M. Megaw and S. Lerman. Application of mini osmotic pump

for liposomal drug delivery to the ocular lens. *Invest. Ophthalmol. Vis. Sci.* **28**:1429–1433 (1987).
12. R. N. Frank, A. Amin, R. Kennedy, and T. C. Hohman. An aldose reductase inhibitor and aminoguanidine prevent vascular endothelial growth factor expression in rats with long-term galactosemia. *Arch. Ophthalmol.* **115**:1036–1047 (1997).
13. L. P. Aiello and J. S. Wong. Role of vascular endothelial growth factor in diabetic vascular complications. *Kidney Int.* **58**:S113–S119 (2000).
14. G. Sunkara, J. DeRuiter, C. R. Clark, and U. B. Kompella. *In vitro* hydrolysis, permeability, and ocular uptake of prodrugs of N-[[4-(benzoylamino)phenyl] sulfonyl]glycine, a novel aldose reductase inhibitor. *J. Pharm. Pharmacol.* **52**:1113–1122 (2000).
15. G. Sunkara, S. P. Ayalasomayajula, C. S. Rao, J. L. Vennerstrom, and U. B. Kompella. Pharmacokinetics of Benzoylaminophenylsulfonylglycine (BAPSG) following intravenous, intraperitoneal, subcutaneous, and oral dosing in rats. *AAPS PharmSci.* **3(suppl.)**: 3 (2001).
16. V. H. L. Lee, K. J. Pince, D. A. Frambach, and B. Martini. Drug delivery to the posterior segment. (ED:Ryan, S.J.). *Retina.* The C.V. Mosby Company. *St. Louis. Chapter* **25**:483–498 (1989).
17. L. Boldrini, A. Calanai, V. Silvestri, F. Basolo, M. Lucchi, A. Mussi, C. A. Angeletti, G. Bevilacqua, and G. Fontanini. Quantitation by competitive PCR assay of vascular endothelial growth factor in non-small cell lung carcinomas. *Int. J. Oncol.* **14**:161–168 (1999).
18. S. Roy and M. Lorenzi. Early biosynthetic changes in the diabetic-like retinopathy of galactose-fed rats. *Diabetologia* **39**:735–738 (1996).
19. L. Shargel and B. C. A. Yu. Pharmacokinetics of drug absorption. *Applied Biopharmaceutics and Pharmacokinetics* (Ed 2). *Appleton Chapter* **7**:114–115 (1985).
20. S. Kobayashi, M. Kasuya, K. Shimizu, Y. Ishii, M. Takehana, K. Sakai, N. Suzuki, and M. Itoi. Glutathione isopropyl ester (YM737) inhibits the progression of X-ray-induced cataract in rats. *Photochem. Curr. Eye Res.* **12**:115–122 (1993).
21. P. J. Hissin and R. Hilf. A fluorometric method for determination of oxidized and reduced glutathione in tissues. *Anal. Biochem.* **74**:214–226 (1976).
22. N. H. Kim, H. H. Jung, D. R. Cha, and D. S. Choi. Expression of vascular endothelial growth factor in response to high glucose in rat mesangial cells. *J. Endocrinol.* **165**:617–624 (2000).
23. K. Naruse, J. Nakamura, Y. Hamada, M. Nakayama, S. Chaya, T. Komori, K. Kato, Y. Kasuya, K. Miwa, and N. Hotta. Aldose reductase inhibitors prevent glucose-induced apoptosis in bovine retinal microvascular pericytes. *Exp. Eye. Res.* **71**:309–315 (2000).
24. S. Sato, L. R. Lin, V. N. Reddy, and P. F. Kador. Aldose reductase in human retinal pigment epithelial cells. *Exp. Eye Res.* **57**: 235–247 (1993).
25. K. C. Dunn, A. E. Aotaki-Keen, F. R. Putkey, and L. M. Hjelmeland. ARPE-19, a human retinal pigment epithelial cell line with differentiated properties. *Exp. Eye Res.* **62**:155–169 (1996).
26. V. N. Reddy, L. R. Lin, F. J. Giblin, M. Lou, P. F. Kador, and J. H. Kinoshita. The efficacy of aldose reductase inhibitors on polyol accumulation in human lens and retinal pigment epithelium in tissue culture. *J. Ocul. Pharmacol.* **8**:43–52 (1992).
27. H. Sone, Y. Kawakami, Y. Okuda, S. Kondo, M. Hanatani, H. Suzuki, and K. Yamashita. Vascular endothelial growth factor is induced by long-term high glucose concentration and upregulated by acute glucose deprivation in cultured bovine retinal pigmented epithelial cells. *Biochem. Biophys. Res. Commun.* **221**: 193–198 (1996).
28. G. Velez and S. M. Whitcup. New developments in sustained release drug delivery for the treatment of intraocular disease. *Br. J. Ophthalmol.* **83**:1225–1229 (1999).
29. A. Sanchez, J. L. Vila-Jato, and M. J. Alonso. Development of biodegradable microspheres and nanospheres for the controlled release of cyclosporin A. *Int. J. Pharm.* **99**:263–273 (1993).
30. R. A. Kowlaru, R. L. Engerman, and T. S. Kern. Abnormalities of retinal metabolism in diabetes or experimental galactosemia VIII. Prevention by amino guanidine. *Curr. Eye Res.* **21**:814–819 (2000).